Flame propagation in a nonuniform mixture: analysis of a slowly varying triple flame

Dold, J W

1989

MIMS EPrint: **2007.87**

Manchester Institute for Mathematical Sciences
School of Mathematics

The University of Manchester

ISSN 1749-9097

COMBUSTION AND FLAME 76: 71-88 (1989)

Flame Propagation in a Nonuniform Mixture: Analysis of a Slowly Varying Triple Flame

J. W. DOLD

School of Mathematics, University of Bristol, University Walk, Bristol BS8 1TW, England

For flames propagating through a nonuniform medium a three-flame structure is described. This consists of a fuel-rich premixed flame, a fuel-lean premixed flame, and, starting where these flames meet, a diffusion flame. Such formations have been observed experimentally and probably occur as laminar flamelets in turbulent diffusion flames. A low-heat-release model for such flame structures is developed and solutions are obtained in the limit of slowly varying premixed flames. Under these conditions, it is shown that the Triple-Flame propagation speed depends on the transverse mixture fraction gradient and is bounded above by the maximum adiabatic laminar flame speed of the system.

INTRODUCTION

The adiabatic laminar flame speed in a uniform medium is strongly dependent on reactant concentrations, and any premixed flame leaves in its wake a uniform residue of combustion products plus an unburned fraction of the rich species. If the medium is nonuniform, the flame speed varies from point to point and the residual unburnt species changes from fuel to oxidant across a stoichiometric boundary. Because the flame speed tends to be greatest at or near any stoichiometric boundary, the flame also tends to surge ahead along the path of this boundary. Away from the boundary, the flames propagate progressively more slowly as they enter regions of weakening mixture strength, whereas in the hot unburned residues of the premixed combustion, fuel and oxidant meet to form a diffusion flame.

Thus three distinct flames can be identified: a fuel-rich premixed flame, leaving unburned fuel behind it; a fuel-lean flame, leaving oxidant; and a diffusion flame along the stoichiometric boundary, beginning where all three flames meet. The leading region of this propagating combustion front may suitably be described as a Triple-Flame [1]. Such flames have been observed experimentally [2, 3], as shown in Fig. 1, and, as transient laminar flamelets, they probably play a role in the combustion of turbulent diffusion flames, where extinction, diffusive mixing, and subsequent reignition of pockets of gas may occur [4]. To date there has been little theoretical work which models this type of flame structure.

In studying steady diffusion flames, Liñán and Crespo considered a fuel and oxidant which mix and react after leaving the end of a splitter plate [5]. They assumed that upstream conduction and diffusion could be neglected. This rules out the possibility of upstream flame propagation, so that substantial burning could only begin through some kind of thermal-runaway ignition process. Subsequent combustion takes the form of transversely propagating premixed flames (which slow down and ultimately extinguish through propagating into regions of weakening mixture ratio) and a diffusion flame that is created as one of these flames crosses a stoichiometric boundary.

With the possible exception of the detailed flame shape near stoichiometry [6], this picture is reasonable provided that the splitter plate itself does not initiate the combustion and provided that

Published by Elsevier Science Publishing Co., Inc.
655 Avenue of the Americas, New York, NY 10010

0010-2180/89/$03.50

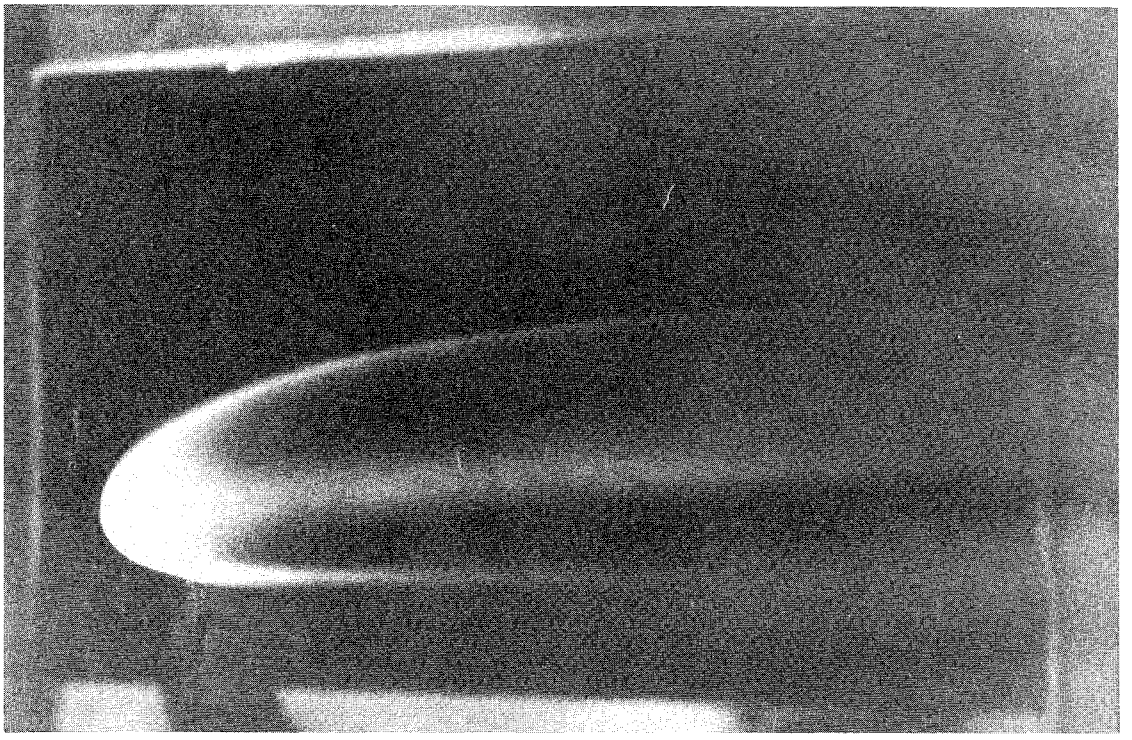

Fig. 1. Triple flame propagating in a nonuniform medium. British Crown Copyright: Reproduced from ref. 2 by kind permission of H. Phillips, Health and Safety Executive, Buxton, U.K.)

the flow speed of the gases exceeds the maximum adiabatic laminar flame speed. For slower flow speeds, upstream conduction and diffusion cannot be neglected; the first onset of substantial combustion in the gases leaving the splitter plate must primarily maintain itself through some kind of upstream flame propagation.

A key factor in determining the structure and propagation speed of a triple flame is the transverse gradient of the mixture fraction that it encounters. For very small gradients, the front of the triple flame is almost flat as it meets an almost uniform medium; the flame then propagates at very nearly the maximum adiabatic laminar flame speed. For increased gradients, the curvature of the front of the flame increases. This reduces the effectiveness of conduction in preheating the gases and so tends to lower the triple flame propagation speed. On the other hand, as observed by Phillips [2], thermal expansion effects behind the curved flame front can modify the flow field ahead of the flame to produce an increase in propagation speed.

For yet larger gradients, the notion of a triple flame begins to fail. For example, with a diffusion flame behind a splitter plate, combustion may begin very close to the plate although probably not quite at the plate [7, 8]. The opportunity for premixing is then so limited that the first onset of combustion may meet such a large transverse mixture gradient that any premixed flames, effectively, merge into the leading end of the diffusion flame. It may be more appropriate to refer to this limiting form of flame structure as a triple point rather than a triple flame [1].

Because it remains stationary, the triple point still retains the property of propagating forwards relative to the oncoming stream of reactants, as it initiates a diffusion flame in its wake. However, the very close proximity of the splitter plate can provide some flame anchoring [8] so that upstream

propagation is not entirely attributable to upstream heat conduction. Indeed, the anchoring may even make it possible for the splitter plate to stabilize a triple point in flow speeds greater than the maximum adiabatic laminar flame speed. In the absence of any form of anchoring, it is not certain that a flame could propagate without distinct premixed flames to initiate the combustion.

A triple-flame structure is therefore possible over some range of transverse gradient of the mixture fracture. In this article a start is made towards modeling this interesting flame structure. As a first step, a simplifying linearization of the convective and conductive–diffusive effects is made by taking the limit of low heat release, giving a nearly constant density model. A large activation energy dependence of the Arrhenius reaction rate on temperature is retained by considering the Zel'dovich number to be large. It is then found that the premixed flames can be considered to be slowly varying if the transverse gradient of the mixture fraction (on the length scale of a typical preheat zone thickness) is small compared with the inverse of the Zel'dovich number.

Realistically, flames do engender significant changes in density. However, it is useful to consider this simplest form of analysis first before proceeding to consider larger temperature increases for which thermal expansion would be more significant. The results still provide a qualitatively valuable description of the nature of triple flames. In cases where the premixed flames are slowly varying, it becomes fairly straightforward to obtain solutions that describe the triple flame at one practically important limit of its parameter space, namely the limit at which the propagation speed is close to the maximum adiabatic laminar flame speed. It is also instructive to derive this model from conditions that, at a later stage, can be used to study other aspects of triple flames.

MODEL

Equations and Nondimensionalization

We consider, for simplicity, the one-step reaction

$$\nu_F F + \nu_X X \rightarrow \nu_P P, \tag{1}$$

in which ν_F fuel molecules and ν_X oxidant molecules produce ν_P product molecules. Fuel and oxidant streams are taken to be originally separated, containing mass fractions Y_{F0} and Y_{X0}, respectively, of fuel and oxidant. We use this to rescale the mass fractions by defining $y_\sigma = Y_\sigma / Y_{\sigma 0}$ for $\sigma = F$ or X so that y_F and y_X vary between 0 and 1. Adopting conventions of unit Lewis number, constant specific heat $\tilde{C}_P$, and low Mach numbers, we consider systems for which a single conserved scalar, which we take to be the mixture fraction Z of fuel, may be used [9]:

$$Z = \left(\frac{Y_F}{\nu_F W_F} + \frac{Y_{X0} - Y_X}{\nu_X W_X} \right) \Big/ \left(\frac{Y_{F0}}{\nu_F W_F} + \frac{Y_{X0}}{\nu_X W_X} \right), \tag{2}$$

where W_σ is the molecular weight of the species σ. The mixture fraction satisfies the evolution equation (for unit Lewis number),

$$\tilde{\rho}(\tilde{\boldsymbol{u}} \cdot \tilde{\nabla}) Z = \tilde{\nabla} \cdot \left(\frac{\tilde{\lambda}}{\tilde{C}_P} \tilde{\nabla} Z \right), \tag{3}$$

where the superscript $\tilde{}$ denotes a dimensional quantity, $\tilde{\rho}$ is the density, $\tilde{\boldsymbol{u}}$ the fluid velocity, and $\tilde{\lambda}$ the thermal conductivity.

The normalized mass fractions y_F and y_X are then given in terms of Z and the absolute temperature $\tilde{T}$ as follows:

$$y_F = Z - \frac{(\tilde{T} - \tilde{T}_0)\tilde{C}_P}{\tilde{Q}\nu_P W_P} \frac{\nu_F W_F}{Y_{F0}}$$

and

$$y_X = 1 - Z - \frac{(\tilde{T} - \tilde{T}_0)\tilde{C}_P}{\tilde{Q}\nu_P W_P} \frac{\nu_X W_X}{Y_{X0}} \tag{4}$$

where $\tilde{T}_0$ is the initial (and, we assume, equal) absolute temperature of the fuel and oxidant streams and $\tilde{Q}$ is the heat of reaction. An upper bound $\tilde{T}_s$ for $\tilde{T}$ is arrived at when both y_F and y_X are zero, so that

$$\tilde{T}_s = \tilde{T}_0 + \frac{\tilde{Q}\nu_P W_P}{\tilde{C}_P \tilde{T}_0} \Big/ \left(\frac{\nu_F W_F}{Y_{F0}} + \frac{\nu_X W_X}{Y_{X0}} \right), \tag{5}$$

when Z takes its stoichiometric value $Z = S$,

where

$$S = Y_{F0}\nu_X W_X/(Y_{F0}\nu_X W_X + Y_{X0}\nu_F W_F). \tag{6}$$

It is natural to nondimensionalize $\tilde{T}$ such that $\tilde{T}/\tilde{T}_s = 1 - (1 - T)\alpha$, where $\alpha = (\tilde{T}_s - \tilde{T}_0)/\tilde{T}_s$. Thus T varies between 1 at its hottest value and 0 well ahead of any flames. This gives the normalized mass fractions as

$$y_F = Z - ST \quad \text{and} \quad y_X = 1 - Z - (1 - S)T. \tag{7}$$

The nondimensional temperature T satisfies the evolution equation

$$\tilde{\rho}(\tilde{\boldsymbol{u}} \cdot \tilde{\nabla})T = \tilde{\nabla} \cdot \left(\frac{\tilde{\lambda}}{\tilde{C}_P}\tilde{\nabla}T\right) + \frac{\tilde{A}\tilde{Q}\nu_P W_P}{\alpha \tilde{C}_P \tilde{T}_s}(\tilde{\rho} y_F Y_{F0})^{\nu_F} \times (\tilde{\rho} y_X Y_{X0})^{\nu_X} \exp\left[\frac{\beta}{\alpha} - \frac{\beta(1-T)}{1-\alpha(1-T)}\right] \tag{8}$$

where β is the Zel'dovich number, $\beta = \alpha\tilde{E}/(\tilde{R}\tilde{T}_s)$, which we assume to be large, $\tilde{E}$ is the activation energy of the reaction, $\tilde{R}$ is the universal gas constant, and $\tilde{A}$ is a preexponential factor which we take to be constant.

We now consider these equations in the broad context of a flow of reactants with diffusive mixing of species governed by Eqs. 3 and 7 and temperature behavior governed by Eq. 8. For a flame propagating steadily in a nonuniform medium this corresponds to choosing a reference frame in which the flame position is fixed. It is appropriate to nondimensionalize velocity against the upstream blowing velocity $\tilde{V}$ (which we shall take to be uniform), and lengths against a conduction–diffusion length scale:

$$\boldsymbol{u} = \tilde{\boldsymbol{u}}/\tilde{V}, \qquad r = \tilde{r}(\tilde{V}\tilde{C}_P\tilde{\rho}_s/\tilde{\lambda}_s), \qquad \rho = \tilde{\rho}/\tilde{\rho}_s \quad \text{and} \quad \tilde{\lambda}/\tilde{\lambda}_s, \tag{9}$$

where $\tilde{\rho}_s$ and $\tilde{\lambda}_s$ are the density and thermal conductivity determined at the temperature upper bound $\tilde{T}_s$ and at ambient pressure. This gives

$$\rho(\boldsymbol{u} \cdot \nabla)Z = \nabla \cdot (\lambda \nabla Z)$$

and

$$V^2[\rho(\boldsymbol{u} \cdot \nabla)T - \nabla \cdot (\lambda \nabla T)] = \beta(\beta\rho y_F)^{\nu_F}(\beta\rho y_X)^{\nu_X} \exp\left[-\frac{\beta(1-T)}{1-\alpha(1-T)}\right], \tag{10}$$

where

$$V^2 = \frac{\tilde{V}^2\alpha\beta}{\tilde{A}} \frac{\tilde{C}_P{}^2\tilde{T}_s\tilde{\rho}_s{}^2}{\tilde{\lambda}_s\tilde{Q}\nu_P W_P} \times (\beta/\tilde{\rho}_s)^{\nu_F + \nu_X} Y_{F0}{}^{-\nu_F} Y_{X0}{}^{-\nu_X} e^{\tilde{E}/(\tilde{R}\tilde{T}_s)}.$$

It can be seen that V varies in direct proportion to $\tilde{V}$ so that increased values of V represent greater blowing velocities. Density ρ and velocity $\boldsymbol{u}$ satisfy the continuity equation and the low-Mach-number version of the ideal gas law

$$\nabla \cdot (\rho \boldsymbol{u}) = 0$$

and

$$[1 - (1 - T)\alpha]\rho = 1 \tag{11}$$

(assuming constant average molecular weight). We also may consider thermal conductivity to be a function of absolute temperature, $\lambda = \lambda[1 - (1 - T)\alpha]$.

Low Heat Release

If we now consider the limit of low heat release, the dependence of these equations on α can be neglected to first order. Density ρ and conductivity λ become unity to first order, and the velocity $\boldsymbol{u}$ stays constant with magnitude unity. We may choose coordinates so that the flow is directed solely along the x axis. Equations 10 then simplify to

$$Z_x = \nabla^2 Z$$

and

$$V^2[T_x - \nabla^2 T] = \beta\mathcal{R}, \tag{12}$$

where

$$\mathcal{R} = \{\beta[Z - ST]\}^{\nu_F}\{\beta[1 - Z - (1 - S)T]\}^{\nu_X} \times e^{-\beta(1-T)}.$$

To determine the controlling properties of the triple flame it is only necessary to consider Z in the region of its stoichiometric value S. The local adiabatic laminar flame speed outside of this range is relatively small, so that the premixed-flame paths are easily described, as was done by Liñán and Crespo [5] and Dold and Clarke [10]. In this article we also restrict attention to small transverse gradients of Z in the region of its stoichiometric value S. Under these circumstances it is feasible to approximate Z locally in the manner

$$Z = S + By/\beta + O(B^2/\beta^2), \tag{13}$$

where $B = \beta Z_{ys}$ and Z_{ys} is the small transverse gradient of Z at the leading end of a triple flame. Also, the origin and orientation of the y axis are normalized so that the stoichiometric boundary lies along the line $y = 0$ (at least locally) and so that we can assume $B > 0$.

It may be noted that $Z = S + By/\beta$ is an exact solution of Eq. 12a, which, physically, would require very specific boundary conditions such as having fixed mixture fractions provided at two parallel plates situated at some positive and negative values of y. The asymptotic form (Eq. 13) arises if Z has nonzero second derivatives, as would more generally be the case. For example, where a splitter plate forces the boundary conditions $Z(-\infty, y < y_0) = 0$, $Z(-\infty, y > y_0) = 1$, and $Z_y(x \le x_0, y_0) = 0$, the solution of Eq. 12a takes the form $Z = 1/2\text{erfc}(-\nu)$ [8], where ν is a parabolic coordinate satisfying $\nu = 1/2(y - y_0)/\sqrt{x - x_0 + \nu^2}$. In this case, Eq. 13 provides a suitable asymptotic form for Z when $x - x_0 = 0(\beta^2/B^2)$.

Boundary conditions require that "ahead" of any premixed flames the temperature T approaches its upstream value of zero. It is assumed that the slow chemical reaction in the gases well ahead of the flame does not have time to significantly alter the upstream temperature before a flame is reached. Despite α being small, we also consider the Zel'dovich number to be large enough to justify using the limit $\beta \to \infty$ in setting up first-order asymptotic solutions for T.

STRUCTURE OF SLOWLY VARYING PREMIXED FLAMES

The analysis of the premixed flames is considerably simplified if they can be considered to be "slowly varying." This effectively permits both the preheat and reaction zones of the flames to be analyzed as parabolic rather than elliptic problems (as in Eq. 12). The analysis will be seen to be justified provided that the parameter B is small, that is, $Z_{ys} \ll \beta^{-1}$. The distinguished limit for which $Z_{ys} \ge O(\beta^{-1})$ will be studied separately.

Use of Flame-Following Coordinates

Let us assume that the reaction zone of the premixed flames lies along the path $x = X(y)$ so that a flame slope can be identified as $\phi = dX/dy$. It is convenient to change coordinates to a set of orthogonal coordinates η and ξ that follow the flame path as shown schematically in Fig. 2. Perhaps the simplest way to construct such a coordinate system is to make use of a complex mapping in the form

$$x + iy = f(\xi + i\eta). \tag{14}$$

It is convenient to build two main features into this transformation. First, in order that the flame path will be given by $\eta \equiv 0$ in the transformed plane, the function f should involve a rotation through an angle of $\cos^{-1}(\phi/\psi)$, where, for brevity, we have written ψ for $\sqrt{(1 + \phi^2)}$. Secondly, the thickness of the preheat zone of the combined fuel-rich and fuel-lean premixed flames (measured on the scale of x and y) will be seen to increase as ψ as $|\phi|$ increases (see Eq. 12). Thus if η is to provide an appropriate coordinate with which to describe the preheat zone, then f should also involve a local scale magnification by a factor of order ψ near the flame. Both of these features are reproduced if the function f is defined such that

$$f(0) = X(0) \quad \text{and} \quad f'(\xi) = \phi(\xi) + i \tag{15}$$

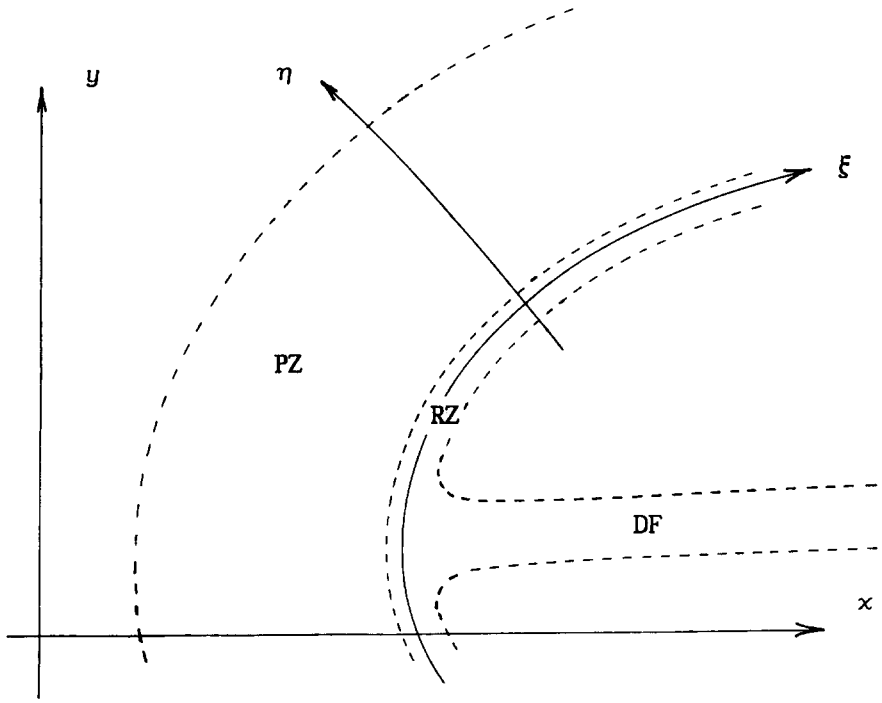

Fig. 2. Structure of a triple flame propagating from right to left, showing the reaction zone (RZ), preheat zone (PZ), diffusion flame (DF), and the transformation to coordinates (η, ξ) which follow the flame path.

on the flame path $\eta \equiv 0$ or $\xi + i\eta = \xi$. As in this boundary condition for f, the flame slope will be considered to be a function of the coordinate that changes along the flame path, namely $\phi = \phi(\xi)$. This definition also sets ξ to zero where the flame meets the stoichiometric boundary at $y = 0$.

The transformation (14) can only be applied if f can be evaluated for nonzero values of η. One way of doing this is to use Eq. 15 to obtain the Taylor series expansions for f' and for f:

$$f'(\xi+i\eta) = \left(\phi - \frac{\eta^2}{2!}\phi'' + \frac{\eta^4}{4!}\phi'''' + \cdots\right) + i\left(1 + \eta\phi' - \frac{\eta^3}{3!}\phi''' + \cdots\right) = \mu + i\omega, \tag{16}$$

and

$$x + iy = X(\xi) + i\xi - \left(\eta + \frac{\eta^2}{2!}\phi' - \frac{\eta^4}{4!}\phi''' + \cdots\right) + i\left(\eta\phi - \frac{\eta^3}{3!}\phi'' + \frac{\eta^5}{5!}\phi'''' + \cdots\right).$$

In terms of μ and ω (the real and imaginary parts of f'), Eqs 12 and 13 lead to the following equation for temperature:

$$\mu T_\xi = \omega T_\eta + T_{\xi\xi} + T_{\eta\eta} + (\mu^2+\omega^2)\beta\mathfrak{R}/V^2,$$

where we take

$$\mathfrak{R} = [(1-T)S\beta + By]^{r_F}[(1-T)(1-S)\beta - By]^{r_X} \times e^{-\beta(1-T)}. \tag{17}$$

Reaction Zone

To model the reaction zone we rescale Z, T, and η in order to highlight the region in which the reaction is most significant, namely when $T = 1 - 0(\beta^{-1})$. Accordingly we define $Z - S = z/\beta = By/\beta$, $1 - T = \Gamma/\beta$, and $\eta = \chi/\beta$ so that, to first order, Eqs. 17 lead to

$$\Gamma_{xx} \sim \psi^2 V^{-2}[S\Gamma + z]^{\nu_F}[(1-S)\Gamma - z]^{\nu_X} e^{-\Gamma},$$

giving

$$\Gamma_\chi^2 \sim 2\psi^2 V^{-2} \times \int_{\Gamma_b(z)}^{\Gamma} (S\gamma + z)^{\nu_F}[(1-S)\gamma - z]^{\nu_X} e^{-\gamma}\, d\gamma, \tag{18}$$

with

$$\Gamma_b(z) = \max\left\{\frac{z}{1-S}, -\frac{z}{S}\right\}.$$

The latter result is obtained using the condition that the temperature slope Γ_χ must tend to zero as Γ approaches its burned value Γ_b (at which the reaction ceases). In particular, as χ becomes large the gradient Γ_χ approaches the finite value

$$\Gamma_\chi(1 \ll \chi \ll \beta) \sim \psi\Omega(z)/V \sim -T_\eta(\xi, \beta^{-1} \ll \eta \ll 1), \tag{19a}$$

with

$$\Omega^2 = 2\int_{\Gamma_b(z)}^{\infty} (S\gamma + z)^{\nu_F}[(1-S)\gamma - z]^{\nu_X} e^{-\gamma}\, d\gamma. \tag{19b}$$

The function Ω is important in providing the matching condition (Eq. 19a), which helps to determine the temperature variation in the preheat zone. A second matching requirement for the preheat zone is that the temperature T should tend to a maximum value of $1 - O(\beta^{-1})$ as η tends to zero.

The integral in Eq. 19 is easily evaluated for integral values of ν_F and ν_X. For example, for the two-body and three-body reactions, $\nu_F = \nu_X = 1$ and $\nu_F = 2$ with $\nu_X = 1$, respectively, $\Omega^2(z; \nu_F, \nu_X)$ becomes

$$\Omega^2(z; 1, 1) = 2 \cdot \begin{cases} [2S(1-S)+z]e^{-z/(1-S)} : z \geq 0 \\ [2S(1-S)-z]e^{z/S} : z \leq 0 \end{cases}$$

and

$$\Omega^2(z; 2, 1) = 2 \cdot \begin{cases} \left[6S^2(1-S) + 4Sz + \dfrac{z^2}{1-S}\right] \\ \quad \times e^{-z/(1-S)} : z \geq 0 \\ [6S^2(1-S) - 2Sz]e^{z/S} : z \leq 0. \end{cases} \tag{20}$$

Sketches of these functions for various values of S are shown in Fig. 3. Because Eq. 19 is invariant under the transformation $S \to 1 - S'$, $\nu_F \to \nu_X'$, $\nu_X \to \nu_F'$, and $z \to -z'$, the three-body reaction $\nu_F = 1$ with $\nu_X = 2$ is given by Eq. 20, with S replaced by $1 - S$ and with the sign of z reversed on the right-hand side. These sketches and appropriate differentiation of Eq. 20 reveal that Ω and $d\Omega/dz$ are continuous functions of z. Further differentiation shows that $d^2\Omega/dz^2$ is also continuous while $d^3\Omega/dz^3$ can be discontinuous at $z = 0$. We will therefore proceed on the assumption that Ω is C^2 continuous at $z = 0$ and C^∞ continuous everywhere else.

We also define Ω_0 as the maximum value of Ω which is found at $z = z_0(S; \nu_F, \nu_X)$, where, in the cases shown in Eq. 20,

$$z_0(S; 1, 1) = \begin{cases} (1-S)(1-2S) : S \leq 1/2 \\ -S(2S-1) : S \geq 1/2 \end{cases}$$

and

$$z_0(S; 2, 1) = \begin{cases} (1-S)\{[(2S-1)^2 + 2S(2-3S)]^{1/2} \\ \quad -(2S-1)\} : S \leq 2/3 \\ -S(3S-2) : S \geq 2/3. \end{cases} \tag{21}$$

It will be seen that the second derivative of Ω at the maximum value, which we denote by Ω_0'', is of fundamental importance in determining the effect of flame curvature on the propagation speed of a slowly varying triple flame. Appropriate differentiation of Eq. 20 leads to

$$\Omega_0\Omega_0'' = \begin{cases} \left[-2+\dfrac{z_0}{(1-S)^2}\right] e^{-z_0/(1-S)} : S\le 1/2 \\ [-2-z_0/S^2]e^{z_0/S} : S\ge 1/2 \end{cases}$$

and

$$\Omega_0\Omega_0'' = \begin{cases} \left[-2(3S-1)-\dfrac{4z_0}{1-S}+\dfrac{{z_0}^2}{(1-S)^3}\right] \\ \quad \times e^{-z_0/(1-S)} : S\le 2/3 \\ [-2(3S-1)-2z_0/S]e^{z_0/S} : S\ge 2/3. \end{cases} \tag{22}$$

As illustrated in Fig. 4, Ω_0'' is nonzero and negative for all permitted values of S.

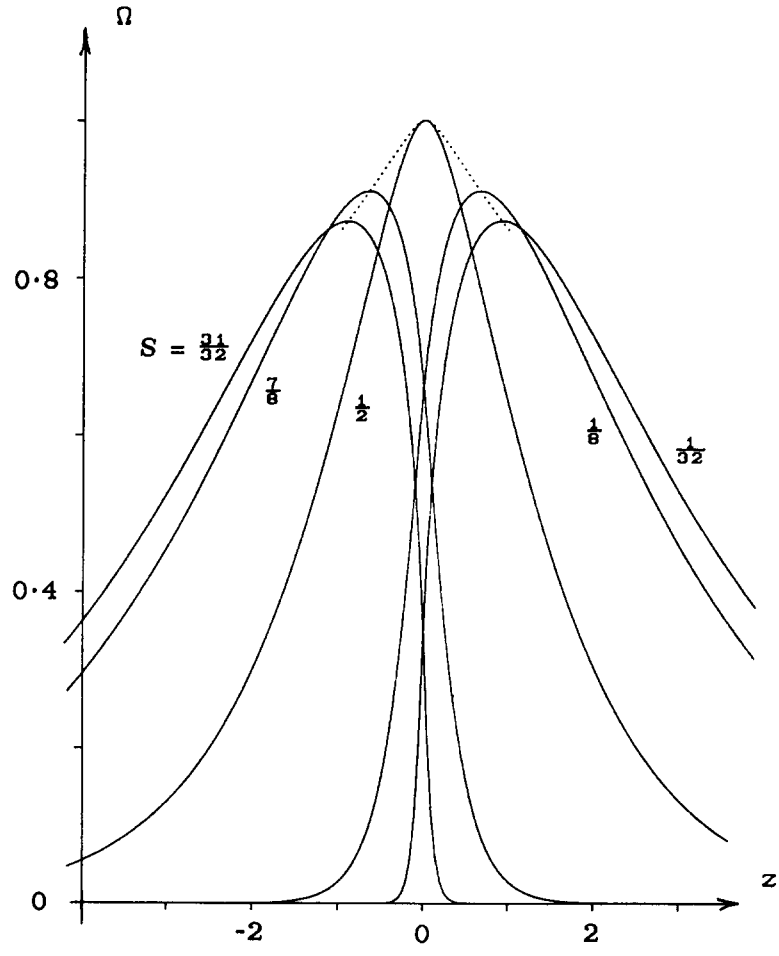

Fig. 3.a. The function $\Omega(z; 1, 1)$ for $S = 1/32$, $1/8$, $1/2$, $7/8$, and $31/32$. The dotted line follows the path of the maximum value of Ω.

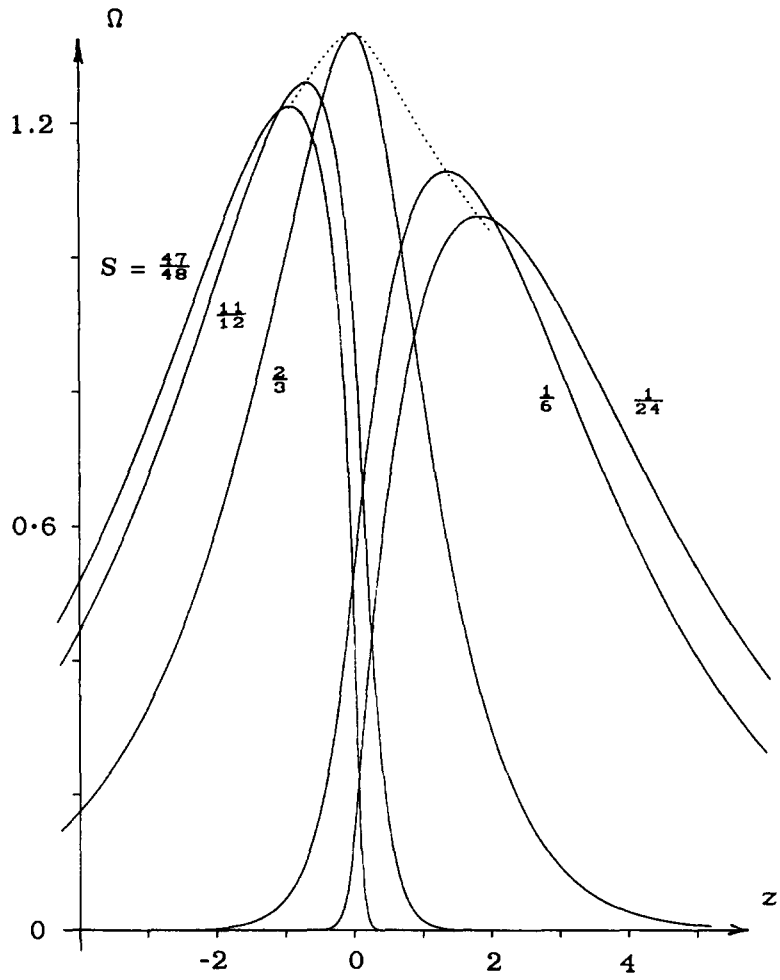

Fig. 3.b. $\Omega(z; 2, 1)$ [as in (a)] for S = 1/24, 1/6, 2/3, 11/12, and 47/48.

Slowly Varying Preheat Zone

In the preheat zone, where T is taken to be strictly less than 1, the reaction-rate term of Eq. 17 becomes exponentially small (and so can be neglected) if β is large. Nevertheless, still being elliptic in nature, Eq. 17 is not readily solved. However, it can be noted that if derivatives with respect to ξ could also be neglected, then the equation would reduce to a relatively simple parabolic differential form. In order to exploit this property, we rescale ξ such that

$$\tau = B\xi. \tag{23}$$

Recalling that z is defined simply as $z = By$, it can be noted from the transformation Eq. 16 that τ is exactly equal to the value of z at positions on the flame path $\eta \equiv 0$. Thus, remembering that the matching condition Eq. 19a varies on the scale of z, it may be anticipated that ϕ and T will vary on the scale of τ. This being so, Eq. 23 shows that derivatives with respect to ξ will only be small if B is small.

Hence, for small values of B, Eq. 17 takes the following form to order B^2 in the preheat zone

$$B\phi T_\tau = (1 + B\eta\dot{\phi})T_\eta + T_{\eta\eta} + B^2 T_{\tau\tau} + O(B^3), \tag{24}$$

where $\dot{\phi}$ denotes the derivative of ϕ with respect to τ. In order to determine the basic structure and behavior of triple flames in their slowly varying limit, we will now solve this equation asymptotically to order B as $B \to 0$. To first order, Eq. 24 has the solution $T \sim e^{-\eta}$ under the conditions that $T \to 0$ ahead of the flames and $T \to 1 - O(\beta^{-1})$ as $\eta \to 0$ and $\beta \to \infty$. Substituting this result back into Eq. 24 leads to the second-order solution

$$T = [1 - B(\eta + \eta^2/2)\dot{\phi}]e^{-\eta} + O(B^2) \tag{25}$$

under the same boundary conditions. This solution shows the effect of flame curvature in that an increasing flame slope (that is, $\dot{\phi} > 0$) leads to a reduction in temperature in the preheat zone.

Shape and Velocity of Premixed Flames

If we now use the solution (Eq. 25) and condition (Eq. 19a) to match the temperature gradient T_η between the preheat and reaction zones, it is found that ϕ must satisfy the asymptotic differential equation

$$B\frac{d\phi}{dz} = \frac{(1+\phi^2)^{1/2}\Omega(z)}{V} - 1 + O(B^2), \tag{26}$$

where we have replaced $d\phi/d\tau$ by $d\phi/dz$ because τ is equal to z on the flame path (or asymptotically equal to z in the matching region). For a proper description of a triple flame propagating from right to left, the flame path $X(y)$ must possess a leading point that may be considered to initiate the

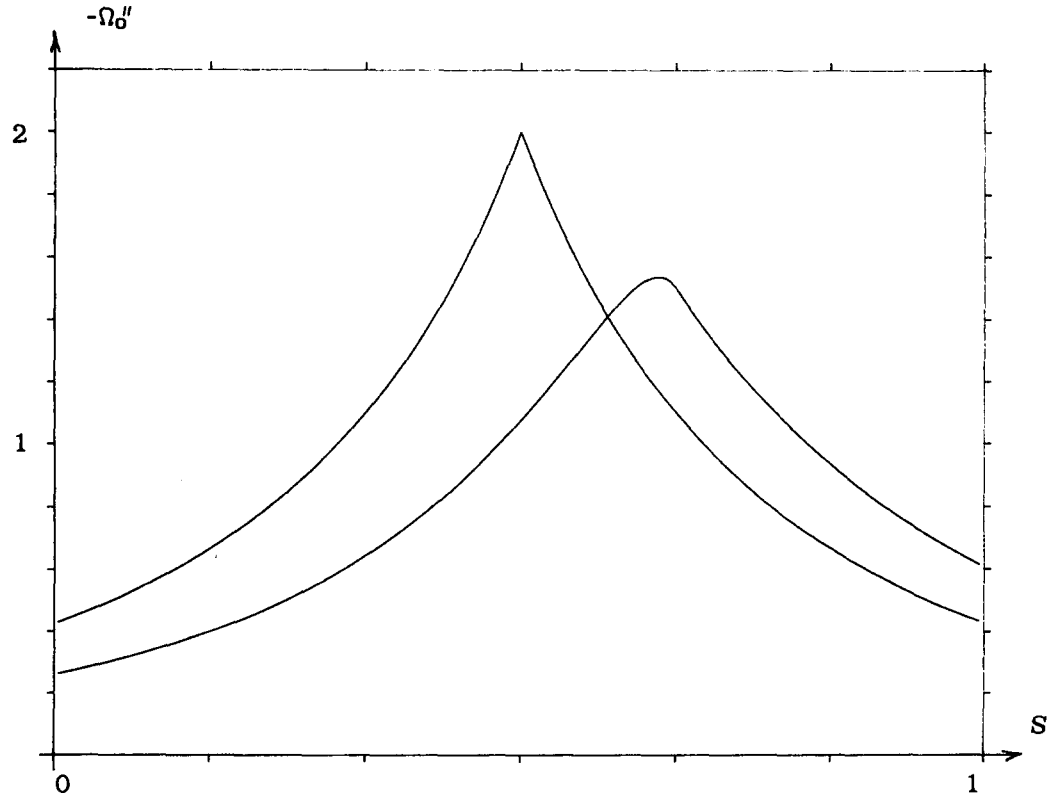

Fig. 4. Values of the second-derivatives at the peak, Ω_0'' (1, 1) and Ω_0'' (2, 1) (the asymmetric curve).

combustion. On either side of this initiating point the premixed flames will tend to trail behind. This can only happen continuously if the flame slope ϕ changes sign at the leading end of the flame, with $\pm\phi > 0$ for large values of $\pm y$ or $\pm z$. This apparently trivial condition is all that is needed to asymptotically solve Eq. 26 for the structure and propagation speed of the leading premixed flames.

Outer Asymptotic Solution

With a little rearranging, Eq. 26 can be written in the form

$$\phi^2 = \frac{V^2}{\Omega^2}\left[1 + 2B\frac{d\phi}{dz} + O(B^2)\right] - 1. \tag{27}$$

nonnegative, but since ϕ must also be equal to zero at least at one point (if ϕ is to change sign continuously), it follows that the minimum value of ϕ^2 must be precisely zero. Applying this condition to Eq. 27 leads to the first-order expression

$$\phi \sim \phi_0(z) = \text{sign}(z - z_0)(\Omega_0^2/\Omega^2 - 1)^{1/2},$$

with

$$V \sim \Omega_0, \tag{28}$$

which shows that $d\phi/dz = \sqrt{(|\Omega_0''|/\Omega_0)} + O(z - z_0)$ near $z = z_0$. Using this to set the minimum value of ϕ^2 to zero at the second order gives

$$\phi \sim \text{sign}(z - z_1)\left\{(\hat{V}/\Omega)^2\left[1 - 2B \times \text{sign}(z - z_0)\frac{\Omega_0^2\Omega'}{\Omega^2}\Big/\sqrt{\Omega_0^2\Omega^2}\right] - 1\right\}^{1/2}, \tag{29a}$$

with

$$V \sim \hat{V} \sim \Omega_0 - B(\Omega_0|\Omega_0''|)^{1/2}, \tag{29b}$$

where z_1 is the position of the minimum value of the quantity enclosed in the brackets { } of Eq. (29a) and $\hat{V}$ is defined so that the value of the minimum is exactly zero. It can be seen that $z_1 = z_0 + O(B)$.

Inner Asymptotic Solution

Equation 29a does not always give sensible results near the leading end of the triple flame. For instance, with $\nu_F = \nu_X = 1$ and $S = 1/2$ the term in the brackets { } has two equal minima so that ϕ cannot be uniquely defined in a neighborhood of $z = z_0$. This reflects a singular nature in the above asymptotic analysis which can be associated with the fact that the first-order differential Eq. 27 is reduced to an algebraic equation at each asymptotic order. This is a typical feature of many singular asymptotic problems. An inner region near $z = z_0$, in which the use of the first derivative may be retained at each asymptotic order, can be identified by defining the new variable $\zeta = (z - z_0)/\sqrt{B}$. Equation 26 then becomes

$$\sqrt{B}\frac{d\phi}{d\zeta} = (1 + \phi^2)^{1/2}\Omega/V - 1 + O(B^2), \tag{30}$$

in which we may take $\Omega \sim \Omega_0[1 - B\Omega_2\zeta^2 + B\sqrt{B}\Omega_3\zeta^3 + O(B^2)]$ with $2\Omega_2 = -\Omega_0''/\Omega_0$ and $6\Omega_3 = \Omega_0'''/\Omega_0$. Since Ω''' is not always continuous at $z = 0$, it should be noted that the value of Ω_3 may change substantially if and when ζ crosses the value $\zeta_0 = -z_0/\sqrt{B}$. This fact becomes especially significant for order one values of ζ_0 [when $z_0 = O(\sqrt{B})$]. If this change happens for nonzero values of ζ_0, the values of Ω_0 and Ω_2 will also need to be varied by amounts of order $B\sqrt{B}$ and $\sqrt{B}$, respectively, to maintain the accuracy of the series expression for Ω. However, such changes are not significant in the orders of asymptotic analysis presented below, for which Ω_0 and Ω_2 may actually be considered to remain uniformly constant.

As before, Eq. 30 has the first-order solution (Eq. 28). To second order we define

$$\phi \sim \phi_0(z_0 + \zeta\sqrt{B}) + B\phi_1(\zeta)$$

and

$$V \sim \Omega_0(1 - BV_1 + B\sqrt{B}V_2) \tag{31}$$

which leads to the following asymptotic form of Eq. 30

$$B\sqrt{B}\left[\frac{d\phi_1}{d\zeta} - \zeta\sqrt{2\Omega_2}\phi_1 + V_2 - \zeta\Omega_3\sqrt{2/\Omega_2}\right]$$

$$= B[V_1 - \sqrt{2\Omega_2}] + O(B^2). \tag{32}$$

To order B this shows that

$$V_1 = \sqrt{2\Omega_2} = (|\Omega_0''|/\Omega_0)^{1/2} \tag{33}$$

which agrees with Eq. 29b for V. At the order $B\sqrt{B}$ the solution for ϕ_1 takes the form

$$\phi_1 = e^{\zeta^2\sqrt{\Omega_2/2}} \int_\zeta^\infty e^{-\xi^2\sqrt{\Omega_2/2}}(V_2 - \xi\Omega_3\sqrt{2/\Omega_2})\, d\xi \tag{34}$$

which satisfies the matching requirement from Eq. 29 that ϕ_1 must be bounded as $\zeta \to \infty$. In those cases for which Ω_3 remains constant for order one values of ζ, this result will only allow ϕ_1 to remain bounded as $\zeta \to -\infty$ if $V_2 = 0$. The solution for ϕ_1 then simply reduces to the constant value $\phi_1 \equiv -\Omega_3/\Omega_2 = \Omega_0'''/(3\Omega_0'')$ for order one values of ζ. It may be noted that the outer solution (Eq. 29) is well behaved under these circumstances and so it is not surprising that the inner solution simply reproduces the inner limit of the outer solution.

In cases for which the leading position of the triple flame z_0 is of order $\sqrt{B}$, the value of Ω_3 may be different on either side of the order one position $\zeta = \zeta_0$. In these circumstances the solution of Eq. 34 becomes either

$$\phi_1 = e^{\zeta^2\sqrt{\Omega_2/2}}\, V_2\sqrt{\pi}(2/\Omega_2)^{1/4}/2$$

$$\times \operatorname{erfc}[\zeta(\Omega_2/2)^{1/4}] - \frac{\Omega_3^+}{\Omega_2}$$

or

$$\phi_1 = e^{\zeta^2\sqrt{\Omega_2/2}} \left\{ V_2\sqrt{\pi}(2/\Omega_2)^{1/4}/2 \right.$$

$$\times \operatorname{erfc}[\zeta(\Omega_2/2)^{1/4}] - \frac{\Omega_3^+ - \Omega_3^-}{\Omega_2}$$

$$\left. \times e^{-\zeta_0^2\sqrt{\Omega_2/2}} \right\} - \frac{\Omega_3^-}{\Omega_2} \tag{35}$$

for $\zeta \geq \zeta_0$ or $\zeta \leq \zeta_0$, respectively, where erfc is the complimentary error function. The terms Ω_3^+ and Ω_3^- denote the values of Ω_3 in the two respective regions. In order for ϕ_1 to remain bounded for negative values of ζ, the term within the brackets { } of the latter result must approach zero as $\zeta \to -\infty$. This leads to the expression for V_2,

$$V_2 = (\Omega_2/2)^{1/4} \frac{\Omega_3^+ - \Omega_3^-}{\Omega_2\sqrt{\pi}} e^{-\zeta_0^2\sqrt{\Omega_2/2}}. \tag{36}$$

In the cases for which Ω was evaluated above, it turns out that $\Omega'''(z; 2, 1)$ is continuous in z so that V_2 is uniformly zero if $\nu_F = 2$ with $\nu_X = 1$. In the case for which $\nu_F = \nu_X = 1$, Ω''' is discontinuous; using the appropriate values, $\Omega_2 = 1$ and $\Omega_3^+ = -\Omega_3^- = 4/3$, the order $B\sqrt{B}$ contribution to the triple flame propagation speed becomes

$$V_2 = 8/[2^{1/4}3\sqrt{\pi}]e^{-z_0^2/(B\sqrt{2})}, \tag{37}$$

which is clearly only significant for values of z_0 of order $\sqrt{B}$.

Sample Numerical Solution

Equation 26 may also be solved numerically. It may be noted from the asymptotic analysis above that the flame slope ϕ must satisfy two distinct boundary conditions for large positive or negative values of z:

$$\lim_{z \to \pm\infty} \phi\sqrt{\Omega/V} = \pm 1. \tag{38}$$

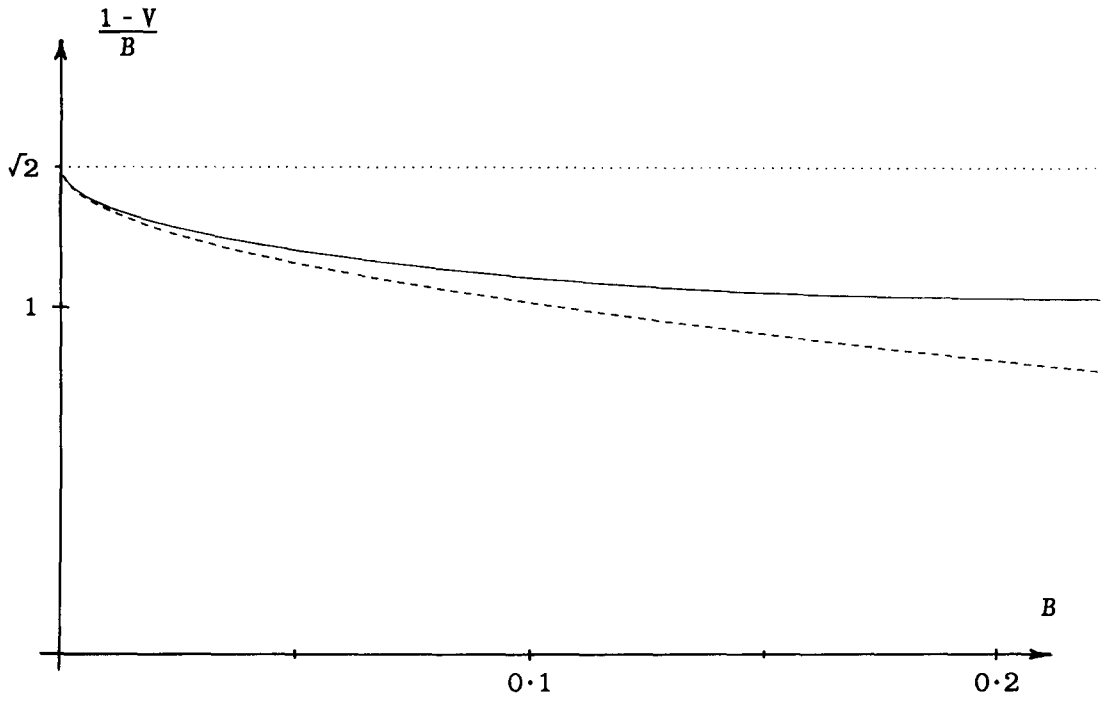

Fig. 5. Numerically calculated flame speed V shown as the ratio $(1 - V)/B$ for $\nu_F = \nu_X = 1$ with $S = 1/2$. The dashed and dotted lines are the asymptotic results to order B and $B\sqrt{B}$, respectively.

This also amounts to the physical requirement that well behind the front of the triple flame, slow premixed flames should propagate transversely with dX/dy asymptotically equal to the flow speed divided by the laminar flame speed. In general, because Eq. 26 is only a first-order nonlinear equation in ϕ, these two conditions cannot both be satisfied for arbitrary values of B and V. However, the two conditions may both be satisfied if B and V satisfy a particular relationship $V = V(B)$ for a given function Ω. Equations 31, 33, and 36 give the asymptotic representation of this relationship to order $B\sqrt{B}$.

Let us consider the simple symmetric example, $\nu_F = \nu_X = 1$, with $S = 1/2$, for which $\Omega^2 = (1 + 2|z|)\exp(-2|z|)$. Because of symmetry we need only use the condition 38 as $z \to +\infty$, with the additional condition that $\phi(0) = 0$. With the $O(B^2)$ term removed, a numerical analysis of Eq. 26 was carried out. By using a shooting method that began with values of ϕ given by the asymptotic relation $\phi \sim \sqrt{V/\Omega}$ for large enough values of z, the unique value of $\phi(0)$ could be accurately calculated for any choice of values of B and V (remembering that B should be small for the slowly varying analysis to be justifiable). Those values of V and B that could be found to give $\phi(0) = 0$ then determine the correct relationship $V(B)$ between the triple-flame propagation speed and transverse mixture gradient, to order B^2.

Results of this analysis are presented in Fig. 5, which shows the relationship between the ratio $(1 - V)/B$ and B for fairly small values of B. It may be noted that $\Omega_0 = 1$ in the example considered. The dashed line is the second-order result from Eq. 33 using the fact that $\Omega_0'' = -2$, while the dotted line is the third-order result obtained using Eq. 37. It can be seen that the numerically computed relationship $V(B)$ closely follows the asymptotic relationship to the order of $B\sqrt{B}$.

Figure 6 shows some examples of the asymptotic triple-flame structures to first and second orders with B set equal to 0·1. The positions of the leading points of the various solutions have been selected so as to keep the curves reasonably separated. In Fig. 7 we show the second-order contributions to ϕ/ψ, calculated using Eq. 29a. As mentioned earlier, the outer solution 29a fails in the case $\nu_F = \nu_X = 1$ with $S = 1/2$, so that the curve for this case has been drawn in two parts for $z < 0$ and $z > 0$ using the third-order inner solution for V in place of $\hat{V}$. The dotted line is the corresponding numerical result. The triple-flame path shown in Fig. 6 for this case was calculated using the numerical solution that can be seen to bridge the gap between the two separate parts of the outer solution.

With the same value of B, Fig. 8 shows the relevant first-, second- and third-order flame speeds as functions of S, using the example solutions 20 for Ω. As expected, the effect of the curvature of the premixed flames near their

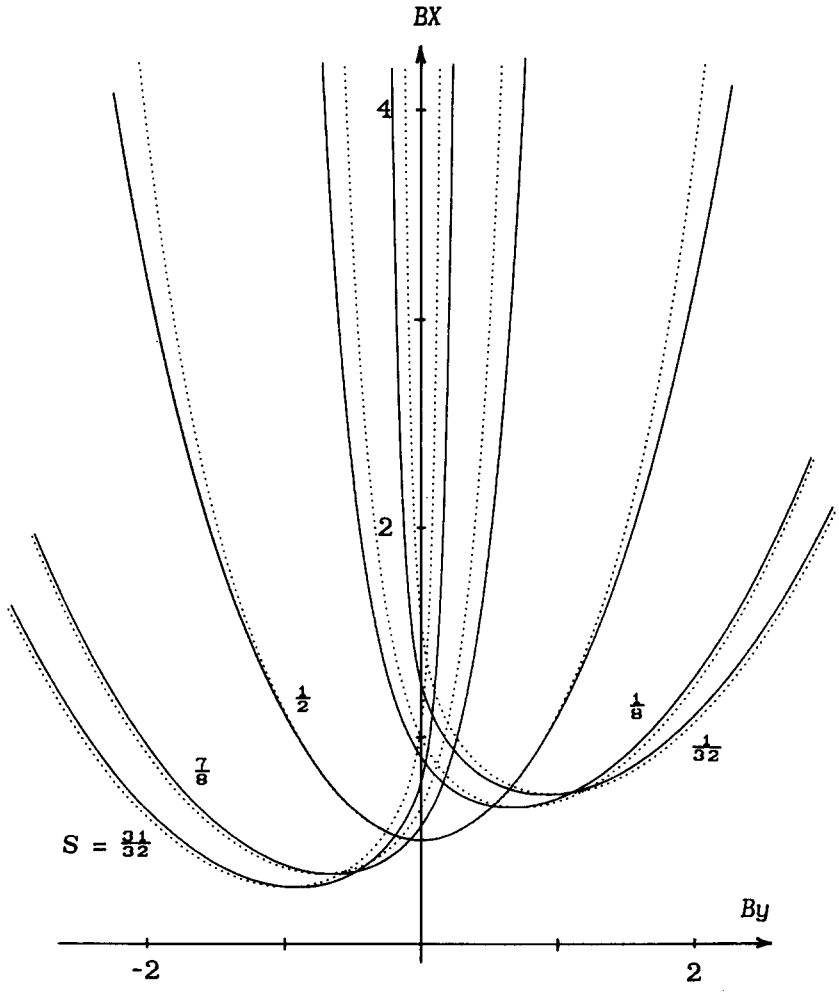

Fig. 6.a. Second-order premixed flame paths of the triple flame for $\nu_F = \nu_X = 1$ with $B = 0{\cdot}1$ and with values of S as in Fig. 3. The dotted lines are the first-order results.

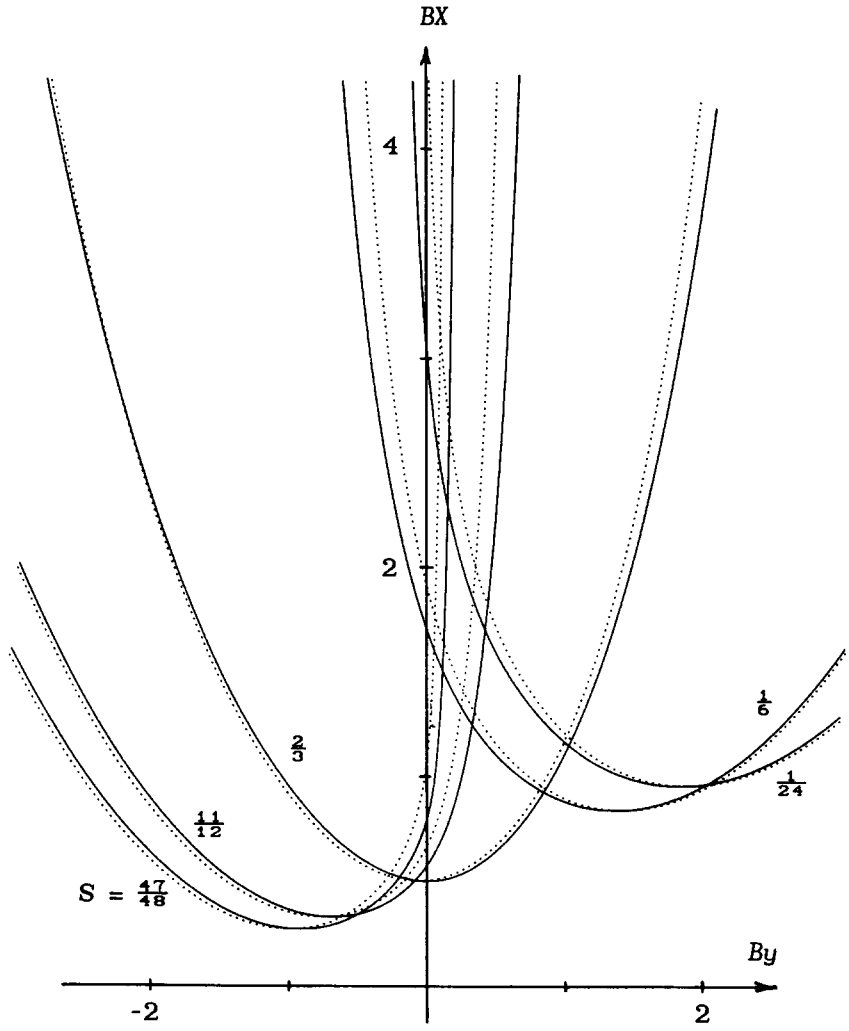

Fig. 6.b. Flame paths as in (a) for $\nu_F = 2$ and $\nu_X = 1$.

leading end is to reduce the triple-flame propagation speed. The influence of the order $B\sqrt{B}$ contribution (shown dotted) is seen to only be relevant over the limited range of values of S that produce order $\sqrt{B}$ values of z_0. The upper bound Ω_0 for V corresponds to the maximum value of the adiabatic laminar flame speed for uniform mixtures that the system could achieve. Indeed, as $B \to 0$ it is clear that the mixture strength in the region of $z = z_0$ tends towards a uniform value which would sustain exactly this flame speed.

DIFFUSION FLAME

Behind the leading premixed flames, the reaction-zone solutions (Eqs. 18) show the temperature T approaching the limiting value,

$$T \sim 1 - \beta^{-1}\Gamma_b(z), \tag{39}$$

which has a discontinuous derivative at the stoichiometric boundary $z = 0$; for $z > 0$, y_X is asymptotically zero, and for $z < 0$, y_F is asymp-

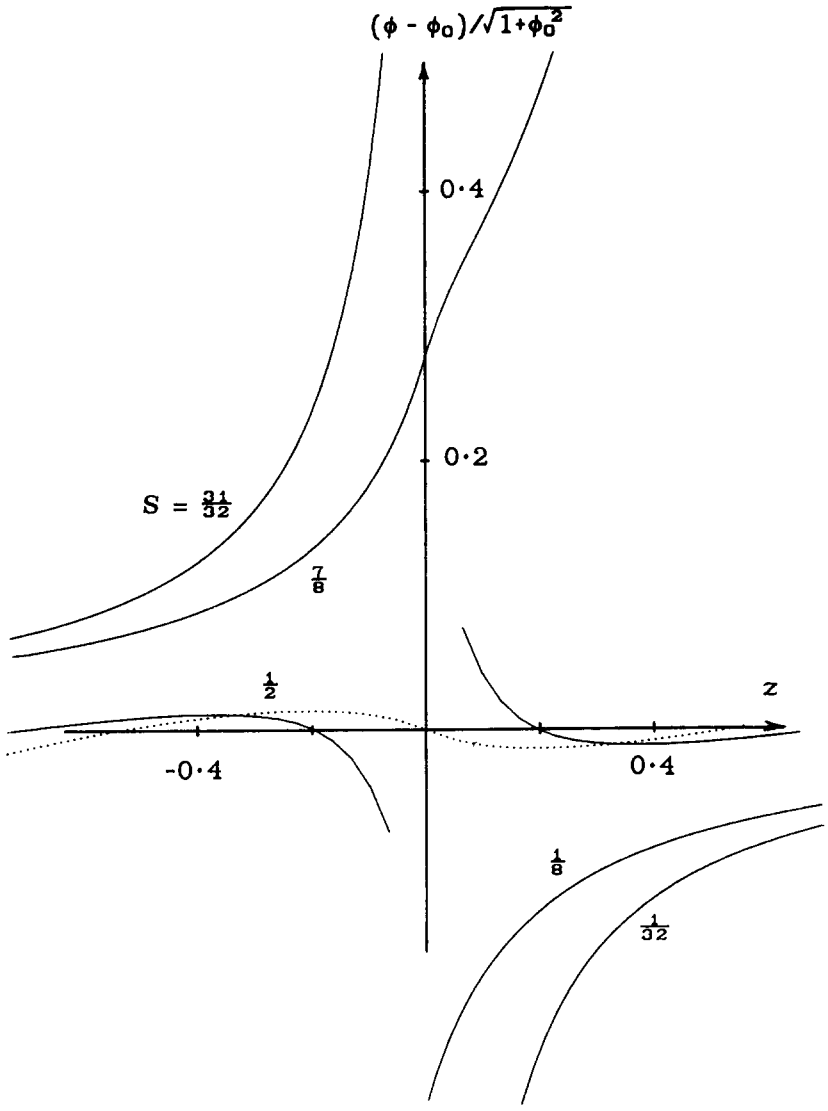

Fig. 7.a.

Fig. 7. a) and b) Second-order contributions to $\phi/\sqrt{1+\phi^2}$ corresponding to the flame paths shown in Fig. 6. The dotted curve is the numerical solution for the case with $\nu_F = \nu_X = 1$ and $S = 1/2$.

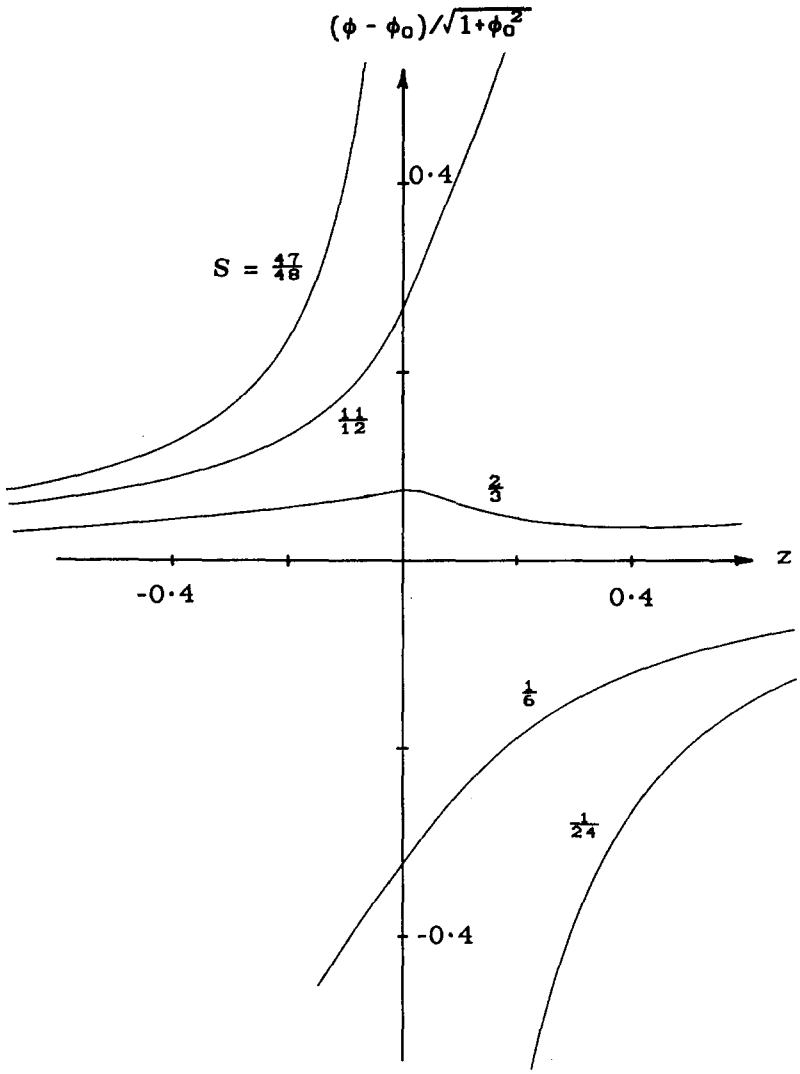

Fig. 7.b.

totically zero. This is the now classical outer solution of a Burke–Schumann diffusion flame, the analysis for which [9] need not be repeated here.

CONCLUSIONS

Having developed a low-heat-release model and obtained solutions in a "slowly varying" limit for the triple flame, it has been demonstrated that a relationship exists between the propagation velocity of a triple flame and the transverse mixture gradient through which the flame propagates. An asymptotic analysis of the premixed flames shows that the propagation speed is mainly dependent on the properties of the reaction zone near the leading end of the triple-flame formation. Under these conditions, the propagation velocity is bounded above by the maximum adiabatic laminar flame speed for the system.

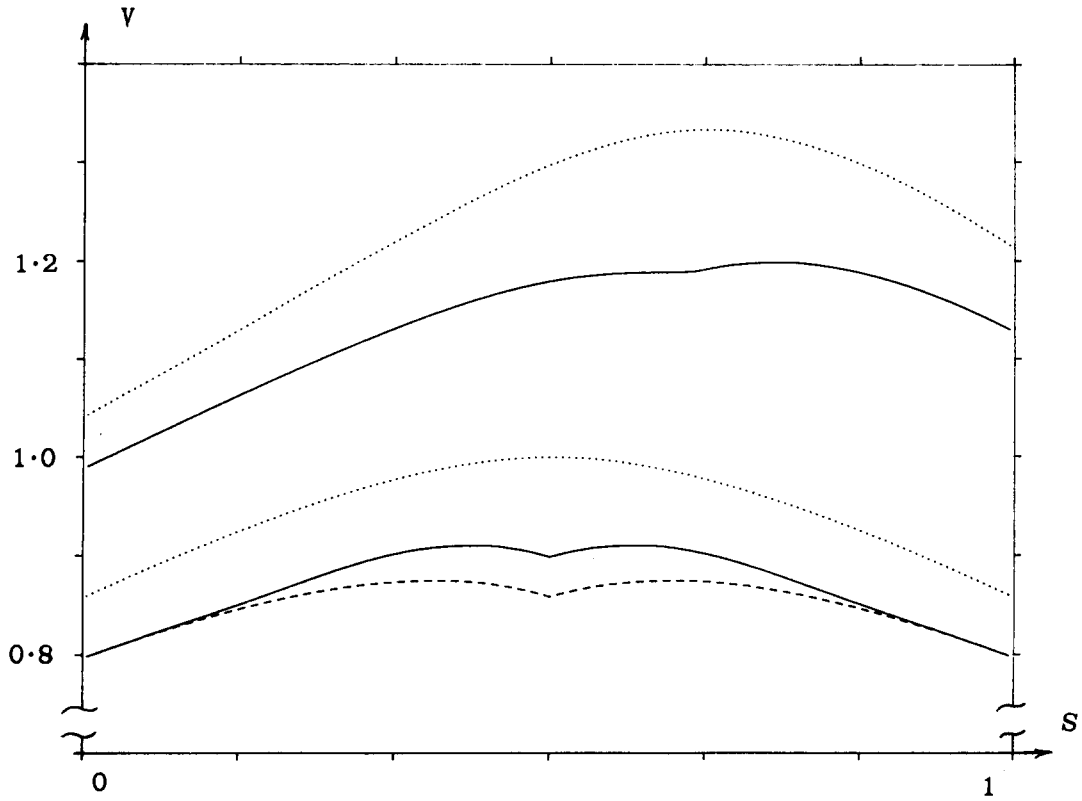

Fig. 8. Third-order flame-speeds with $B = 0{\cdot}1$. The first-order results are shown in dashed lines and the second-order in dotted lines. The upper set of curves applies to the case with $\nu_F = 2$ and $\nu_X = 1$, and the lower set to $\nu_F = \nu_X = 1$.

Financial support for this work was provided by the Science and Engineering Research Council as part of its initiative for funding Nonlinear Studies. The author is particularly grateful to Bernd Rogg and John Clarke for valuable discussions about the problem, and to Prof. F. A. Goldsworthy, whose suggestions led towards a deeper understanding of the analysis.

REFERENCES

1. Rogg, B., Clarke, J. F., and Peters, N., private discussions, 1986.
2. Phillips, H., *Flame in a Buoyant Methane Layer*. 10th International Symposium on Combustion, Cambridge 1965, pp. 1277–1283.
3. Ishizuka, S., private communication, 1986.
4. Peters, N., *Laminar Flamelet Concepts in Turbulent Combustion*. 21st International Symposium on Combustion, Munich 1986.
5. Liñán, A. A., and Crespo, A., *Asymptotic Analysis of Unsteady Diffusion Flames for Large Activation Energies*. Combust. Sci. Technol. 14, 95, 1976.
6. Dold, J. W., *Flame Propagation in a Non-Uniform Mixture: The Structure of Anchored Triple-Flames*. 11th International Colloquium on Dynamics of Explosions and Reactive Systems, Warsaw 1987; to be published.
7. Melvin, A., Moss, J. B., and Clarke, J. F., *Streamwise Deflection by a Diffusion Flame. Comb. Sci. Technol.* 6:135–142, 1972.
8. Clarke, J. F., *Diffusion Flame Downstream of an Insulated Splitter-Plate or Partition*. Private communication, 1987.
9. Williams, F. A., Combustion Theory. Benjamin Cummings, Merlo Park, CA, 1985.
10. Dold, J. W., and Clarke, J. F., *Combustion of a Finite Quantity of Gas Released in the Atmosphere*, 21st International Symposium on Combustion, Munich, 1986, to be published.

Received 1 July 1987; revised 10 June 1988